Microscopy and Microanalysis, **31** (7), 2025, 269–270
https://doi.org/10.1093/mam/ozaf048.138

Microscopy AND Microanalysis

Proceedings

Exploring the Chemical and Structural Complexity of Far-From-Equilibrium Oxi-Carbo-Nitride Nanoprecipitates in Additively Manufactured Steels

Amir R. Farkoosh[1,2,*], Roberto dos Reis[1,4], Dieter Isheim[1,2], Vladimir Popov[3], Noam Eliaz[3], and David N. Seidman[1,2]

[1]*Department of Materials Science and Engineering, Northwestern University, Evanston, IL, USA*
[2]*Northwestern University Center for Atom-Probe Tomography (NUCAPT), Evanston, IL, USA*
[3]*Department of Materials Science and Engineering, Tel-Aviv University, Ramat Aviv, Tel Aviv, Israel*
[4]*Northwestern University Atomic and Nanoscale Characterization Experimental (NUANCE) Center, Northwestern University, Evanston, IL, USA*

*Corresponding author: Farkoosh@northwestern.edu

Selective laser melting (SLM), a powder bed fusion additive manufacturing (AM) technique, utilizes a high-power laser to selectively melt and fuse metal powders layer-by-layer, enabling far-from-equilibrium micro-/nano-structures, unattainable via conventional manufacturing [1]. The inherent large surface-to-volume ratio of the powder feedstock, produced through inert gas atomization, increases susceptibility to oxygen and nitrogen contaminants. Gas-atomized steel powders typically contain ~200 wt. ppm (~700 at. ppm) oxygen and, depending on processing conditions, nitrogen concentrations as high as ~1000 wt. ppm (~4000 at. ppm). Due to the low solubility of oxygen in iron, it predominantly forms oxide phases with oxygen-gettering elements present in a steel, such as Si, Mn, Mg, Zr, Al, and Ti. The presence of macro-scale oxide inclusions is of significant concern, as they can deteriorate mechanical properties due to weak cohesion at metal/inclusion heterophase interfaces. While oxygen levels are strictly controlled (<20 wt. ppm) in conventional manufacturing, the inevitably higher oxygen content in AM powders raises concerns about its impact on mechanical performance. Additionally, the residual nitrogen present in the powder feedstock is usually retained in steels after processing, which significantly influences phase stability, microstructure, and mechanical properties, further complicating AM processing. Effective mitigation strategies involve alloying with strong nitride-forming elements, such as Ti and Nb to de-nitride AM microstructures.

Recently, QuesTek Innovations LLC developed QT17-4+, a stainless steel specifically designed for AM, based on modifications made to a conventional precipitation-hardened 17-4PH steel. Prior investigations indicate that this martensitic stainless steel demonstrates relatively consistent microstructures and good mechanical properties when processed additively using a wide range of processing parameters and impurity concentrations [2]. The formation of complex O- and N-rich nanoprecipitates was confirmed within the matrix. In this study, we leverage three-dimensional atom-probe tomography (3D-APT) and four-dimensional scanning transmission electron microscopy (4D-STEM) to elucidate the formation of structurally and chemically complex metastable nanoprecipitates in QT17-4+ for SLM solidification conditions. While 3D-APT provides sub-nanoscale structural and chemical insights, 4D-STEM offers detailed crystallographic information at near-atomic length scales, enabling a comprehensive understanding of nanostructure. Furthermore, we assess whether these nanoprecipitates exhibit partial or complete crystallinity or are amorphous, as their structure directly influences cohesive energies at heterophase interfaces and their impacts on mechanical properties.

QT17-4+ steel powders were produced by argon gas atomization and processed using SLM in an argon environment with less than 0.2 vol.% oxygen. The SLM process was performed on a commercial DMG MORI LASERTEC 12 SLM (LT 12 SLM) machine (DMG MORI, Bielefeld, DE) after determining the optimal processing parameters. Focused ion beam (FIB)-prepared lamellas of the 3D-printed specimens were studied employing an energy filtered 4D-STEM (EF-4D-STEM) approach with a near-parallel electron probe (convergence angle of 0.75 mrad) using a JEOL ARM300F(S)TEM equipped with a Gatan Imaging Filter (GIF) Continuum spectrometer coupled to a K3 IS direct electron detector. The open-source py4DSTEM software package was employed for 4D-STEM data analyses [3]. Nanotips for APT investigations were prepared by cutting ~0.3×0.3×10 mm^3 blanks from the SLM-processed specimens, followed by a two-step electropolishing technique [4]. 3D-APT experiments were performed utilizing a laser-pulsed local-electrode atom-probe LEAP5000XS tomograph (Cameca Instruments Inc., Madison, WI) at a base temperature of 60 K in ultrahigh vacuum ($<10^{-8}$ Pa). Picosecond ultraviolet (UV) laser pulses (wavelength = 355 nm) were applied with an energy of 30 pJ per pulse and a pulse repetition rate of 500 kHz, while maintaining an average detection rate of 2-6%. Data analyses were performed using the program IVAS 3.8.2 (Cameca, Madison, WI). LEAP tomographic datasets were reconstructed using the voltage model.

Typical for an auto-tempered martensitic structure, carbon-rich features (predominantly carbon-decorated dislocations and inter-lath boundaries, or epsilon carbides) are often observed in the as-printed steel, Fig. 1. Additionally, our APT analyses reveal the formation of "*Ti/Al-oxy-carbo-nitride*" nanoprecipitates (D ~ 20-30 nm) exhibiting a complex core-shell morphology, Fig. 2a. 4DSTEM analyses suggest that these complex nanoprecipitates are made of smaller crystals (D ~ 2-5 nm), mainly of Al-rich and Ti-rich phases. These nanoscale oxy-carbo-nitrides remove oxygen and nitrogen impurities introduced during the atomization and printing processes from the matrix. Creating an inventory of these micro/nano-structural features is of great interest as it enables us to understand the solidification paths, phase transformations and strengthening mechanisms, as well as identifying potential hydrogen trapping sites within the far-from-equilibrium microstructures [5].

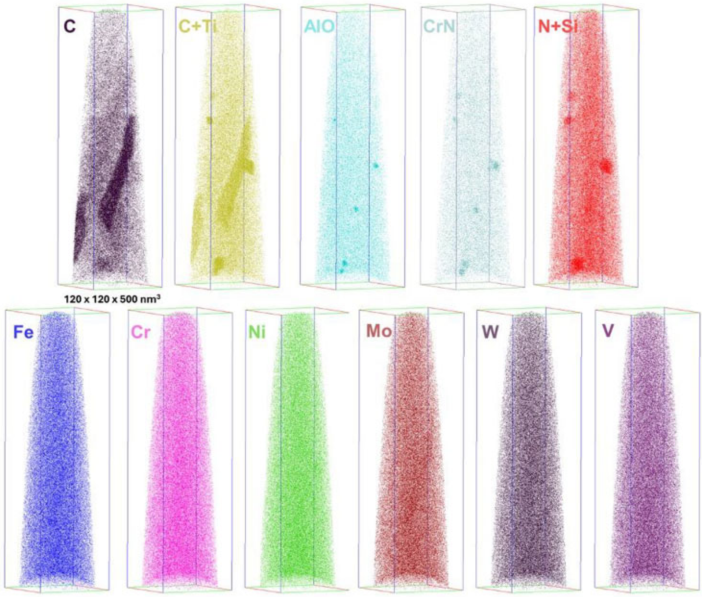

Fig. 1. 3D-APT reconstructions of an SLM-processed QT17-4+ stainless steel (Fe-14Cr-5Ni-0.17C-0.5W-0.08V-0.16Ti, wt.%), displaying the distribution of elements within the nanostructure. A total of 310 M atoms is collected in this dataset utilizing a LEAP 5000XS tomograph. For the structures of the Ti- and N- rich features see Fig. 2.

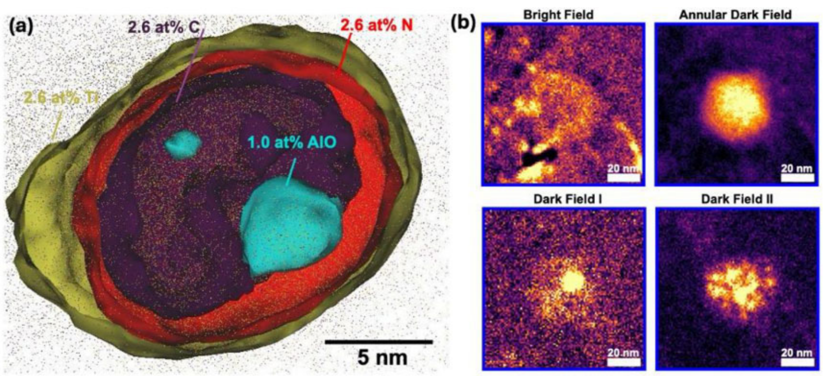

Fig. 2. (a) 3D-APT reconstruction of a structurally and chemically complex Ti/Al-oxy-carbo-nitride nanoprecipitate formed in an SLM-processed QT17-4+ steel. Four different isoconcentration surfaces are used to reveal the chemical complexity of this nanoprecipitate. These nanoprecipitates form during solidification, effectively de-oxidizing, and de-nitriding the melt pool leading to a more reliable microstructure and improved mechanical properties. (b) 4D-STEM analyses of a similar Ti/Al-Oxy-Carbo-Nitride nanoprecipitate in the same steel, displaying virtual bright-field, annular dark-field, and two different dark-field micrographs reconstructed using the py4DSTEM software package. The dark-field I is reconstructed from the Bragg reflections of a corundum (Al_2O_3) phase, while dark-field II is reconstructed from the reflections of a phase best indexed as cubic Ti(C,N).

References

1. Herzog D *et al. Acta Materialia* (2016) **117** 371-392. https://doi.org/10.1016/j.actamat.2016.07.019
2. Sharma VM *et al. Advanced Materials Technologies* (2024) **9** 2400024. https://doi.org/10.1002/admt.202400024
3. Savitzky BH *et al. Microscopy and Microanalysis* (2021) **27** p. 712. https://doi:10.1017/S1431927621000477
4. Krakauer BW and Seidman DN. *Review of Scientific Instruments* (1992) **63** 4071-4079. https://doi.org/10.1063/1.1143214
5. This research was supported by an NSF-BSF grant (DMR 2105362): Dr. Jonathan D. Madison serving as the grant officer. We would like to acknowledge the support and valuable information provided by QuesTek Innovations LLC on the QT17-4+ steel. Atom-probe tomography was performed at the Northwestern University Center for Atom-Probe Tomography (NUCAPT). The local-electrode atom-probe (LEAP) tomograph utilized in this research was purchased and upgraded with funding from NSF-MRI (DMR-0420532), ONR-DURIP (N00014-0400798, N00014-0610539, N00014-0910781, N00014-1712870, N00014-2312593), and DURIP-ARO (W911NF2110052) programs. NUCAPT received support from the MRSEC program (NSF DMR- 2308691) at the Materials Research Center, the SHyNE Resource (NSF ECCS-2025633), and the Initiative for Sustainability and Energy (ISEN) at NU. This work made use of the EPIC facility of the NUANCE Center, which has received support from the MRSEC program (NSF DMR-2308691) at the Materials Research Center; the International Institute for Nanotechnology (IIN NIH-S10OD026871); and the State of Illinois, through the IIN. This research was supported in part through the computational resources and staff contributions provided for the Quest high-performance computing facility at Northwestern University, which is jointly supported by the Office of the Provost, the Office for Research, and Northwestern University Information Technology.